Research Article

Zedong Qiu#, Limin Deng#, Shuang Lu*, Guoqiang Li*, and Zhen Tang

Effect of LDH on the dissolution and adsorption behaviors of sulfate in Portland cement early hydration process

https://doi.org/10.1515/rams-2022-0039
received March 06, 2022; accepted April 04, 2022

Abstract: In recent years, it has been widely recognized that the incorporation of Mg–Al–LDH into cement-based materials can improve the salt corrosion resistance of cement-based materials. The reason for the improvement comes from the anion adsorption capacity of Mg–Al–LDH. It was confirmed that the addition of Mg–Al–LDH would accelerate the setting and hardening of cement paste. With the increase in the Mg–Al-LDH content, the initial setting time of cement slurry with different gypsum contents will decrease by 10–50% and the viscosity of the cement slurry will increase by 100–200%. Depending on different gypsum contents, the degree of cement hydration varied. This article also found that the gypsum in the cement has a negative effect on the resistance to salt erosion, which was brought about by the Mg–Al-LDH adsorption capacity.

Keywords: LDH, gypsum, early hydration of cement, corrosion resistant

1 Introduction

With the continuous development of the field of civil engineering, the research on the durability of concrete has gradually drawn more and more attention, especially revolving around the durability research of sulfate corrosion. With the infiltration and corrosion of SO_4^{2-}, Afm in concrete will be transformed into Aft, resulting in the expansion and cracking of concrete. How to improve the sulfate corrosion resistance of concrete has become one hot research direction in the field of concrete materials.

Layered double hydroxide (LDH) is a relatively new material, which has a wide range of applications in the fields of environment, chemistry, biology, and energy. Its general structural formula is $[M^{2+}_{1-x}M^{3+}_x(OH)_2]^{x+}(A^{n-})_{x/n}{\cdot}mH_2O$ [1] and its most common form in nature is Mg–Al-LDH. In recent years, Mg–Al-LDH has been incorporated into concrete to study its effect on the improvement of concrete resistance to chloride corrosion and sulfate corrosion, due to LDH's unique interlayer anion exchangeability in a solution environment ($CO_3^{2-} > SO_4^{2-} > OH^- > F^- > Cl^- > Br^- > NO_3^-$ [2–4]). There are many ways to synthesize Mg–Al-LDH, ranging over coprecipitation method, sol–gel method, hydrothermal synthesis method, ion exchange method, structure reconstruction method, mechanochemical method, etc. The particle size, crystallinity, and adsorption performance of LDH of different synthesis methods will also be different [5]. LDH has the function of structural reconstruction after high-temperature calcination. LDH after high temperature calcination is called LDO [6].

Later, Mg–Al-LDH was incorporated into cement-based materials as an anionic adsorbent. Studies have confirmed that the incorporation of Mg–Al-LDH into cement-based materials can enhance the ability of cement-based materials to resist sulfate corrosion and carbonate salt corrosion. In the pore solution simulating alkali-activated slag cement, Mg–Al-LDHs were bound to chloride ions through surface adsorption and ion exchange, which accounted for 90 and 10% of the total bound ions, respectively [7]. Shui et al. [8]

# Zedong Qiu and Limin Deng contributed equally to this work.

*** Corresponding author: Shuang Lu,** School of Civil Engineering, Harbin Institute of Technology, 150090, Harbin, China; Key Lab of Structures Dynamic Behavior and Control of the Ministry of Education, Harbin Institute of Technology, 150090, Harbin, China, e-mail: lus@hit.edu.cn
*** Corresponding author: Guoqiang Li,** The Architectural Design and Research Institute of HIT, Harbin 150090, China, e-mail: liguoqiangabc@163.com
Zedong Qiu, Zhen Tang: School of Civil Engineering, Harbin Institute of Technology, 150090, Harbin, China; Key Lab of Structures Dynamic Behavior and Control of the Ministry of Education, Harbin Institute of Technology, 150090, Harbin, China
Limin Deng: The Association of Shanghai Internet Financial Industry, 201399, Shanghai, China

found that the incorporation of Mg–Al-LDH can improve the chloride ion-binding capacity of cement paste, and theoretically proved that the incorporation of Mg–Al-LDH can delay the corrosion of steel bars by chloride salts in concrete. Yang et al. [9] confirmed that the incorporation of Mg–Al-LDHs reduced the diffusion rate of chloride ions in the mortar, and there is no obvious negative effect on the mechanical strength of the mortar. By testing the chloride equilibrium isotherm, corrosion potential, and polarization resistance of steel, Xu et al. [10] confirmed that the incorporation of LDH in a saturated calcium hydroxide solution environment can inhibit the corrosion of steel. Tatematsu and Saski [11] added LDH to prepare the concrete specimen, and proved that the long-term corrosion inhibition effect of LDH on steel is effective. Qu et al. [12] also confirmed the effect of LDH particle size and dosage on the chloride ion penetration resistance of cement-based materials through experiments. In addition to slowing down the corrosion of steel bars in concrete, LDH can improve the sulfate and carbonate resistance of cement-based materials [13–16].

While LDH improves the corrosion resistance of cement-based materials to inorganic salts, it also affects other properties of cement-based materials. Many scholars have found through experiments that the compressive strength of cement-based materials will decrease with the addition of the content of Mg–Al-LDH [4,14,17]. These findings support that Mg–Al-LDH does not participate in the hydration reaction in cement-based materials, which will create new weak interfacial regions. However, the addition of Ca–Al-LDH and LDO can improve the compressive strength of cement-based materials [12,18,19]. On the one hand, Ca–Al-LDH promotes the hydration reaction, and on the other hand, the high level of water absorption of Ca–Al-LDH and LDO reduce the water–cement ratio. Most of the research shows that the addition of LDH can significantly reduce the setting time of cement-based materials [13,18,20], with the increase of LDH content, the setting time is shortened further. Reasons behind this would vary depending on the type of LDH. Nanomaterials can shorten the setting time of cement-based materials and Ca–Al-LDH will form seeds in the cement paste to shorten the setting time. The reason for which Mg–Al-LDH shortens the setting time mainly depends on its interlayer anion. The type of interlayer anion determines whether Mg–Al-LDH will have water absorption and inhibitory effect on gypsum.

Mg–Al-LDH has a great influence on the early hydration process of cement paste because of the water absorption properties and the adsorption capacity of Mg–Al-LDH. The improvement of the corrosion resistance of cement paste by Mg–Al-LDH is mainly due to its anion adsorption capacity. In theory, the SO_4^{2-} of gypsum in cement plays a negative role in the corrosion resistance of Mg–Al-LDH. The proposed study focuses on the effect of two different anion-based Mg–Al-LDH on the early hydration process of cement paste and explores the interaction between Mg–Al-LDH and gypsum in cement during cement hydration.

2 Materials and methods

2.1 Synthesis of Mg–Al–NO_3^--LDH and Mg–Al–CO_3^{2-}-LDH

The method used for synthesizing Mg–Al-LDH in this article was the urea synthesis method.

In this experiment, according to the mixing ratio, 31.73 g $Mg(NO_3)_2{\cdot}6H_2O$, 23.24 g $Al(NO_3)_3{\cdot}6H_2O$, 50 g $CO(NH_2)_2$, and 10.7 g NH_4NO_3 were poured into beakers, then added deionized water to each beaker, and stirred and dissolved to 50 mL. The four solutions were mixed and stirred at 40°C under nitrogen atmosphere for 4 h. Then let the mixture react at 90°C for 40 h. The obtained sample was fully washed with deionized water to pH 7 and then washed again to ensure that the residual urea in the sample is fully washed at 25°C. The washed filter cake was put into an oven to dry and grinded it to obtain Mg–Al–NO_3^--LDH.

The synthesis method of Mg–Al–CO_3^{2-}-LDH is similar to that of Mg–Al–NO_3^--LDH, except that the reactants are changed to 14.9 g $MgSO_4$, 42.46 g $Al_2(SO_4)_3$, 50 g $CO(NH_2)_2$, and 10.7 g $NaHCO_3$.

2.2 Test of SO_4^{2-} adsorption performance of Mg–Al–NO_3^--LDH and Mg – Al – CO_3^{2-}-LDH

The SO_4^{2-} adsorption experiments in this article comprise adsorption kinetics experiments and adsorption isotherm experiments.

2.2.1 Adsorption kinetic experiments

The 0.2 g Mg–Al-LDH was added to 50 mL of the 5 mmol·L^{-1} Na_2SO_4 solution and put it into a shaking bed for shaking at a shaking speed of 240 rpm. After shaking at different times, the centrifuge tube was allowed to stand and 3 mL of the supernatant was taken. The supernatant was filtered with a 0.22 μm membrane filter, and the ion concentration of SO_4^{2-} in the filtrate was measured by an ion chromatography. Each of the above experiments was repeated three times

and the mean value is given as the result. The obtained results were fitted with pseudo-first-order kinetic model (1) and pseudo-second-order kinetic model (2), respectively [21].

$$\ln(q_e - q_t) = \ln q_e - k_1 t, \quad (1)$$

$$t/q_t = 1/(k_2 q_e^2) + t/q_e, \quad (2)$$

where k_1 (min^{-1}) and k_2 [$g\cdot(mg\cdot min)^{-1}$] are the adsorption rate constants, respectively, and q_e and q_t ($mg\cdot g^{-1}$) represent the adsorption capacity at equilibrium and time t, respectively.

2.2.2 Adsorption isotherm experiments

The 0.2 g Mg–Al-LDH was added to 50 mL of Na_2SO_4 solution of different concentrations and put it into a shaking bed for shaking at a shaking speed of 240 rpm. After shaking for 3 h, the centrifuge tube was allowed to stand and 3 mL of the supernatant was taken. The supernatant was filtered with a 0.22 μm membrane filter, and the ion concentration of SO_4^{2-} in the filtrate was measured by an ion chromatography. Each of the above experiments was repeated three times and the mean value is given as the result. The obtained results were fitted with Langmuir isotherm model (3) and Freundlich isotherm model (4), respectively [21].

$$q_e = K_L Q C_e/(1 + K_L C_e), \quad (3)$$

$$q_e = K_f C_e^n, \quad (4)$$

where K_L ($L\cdot mg^{-1}$) and K_f ($mg^{(1-n)}L^n\cdot g^{-1}$) are the Langmuir adsorption constant and the Freundlich affinity coefficient, respectively; Q ($mg\cdot g^{-1}$) is the maximum adsorption capacity; C_e ($mg\cdot L^{-1}$) is the concentration of adsorbate at equilibrium; and n is the Freundlich linearity constant.

2.3 Cement paste specimens

To compare and evaluate the interaction between Mg–Al-LDH and gypsum in cement paste, cement paste specimens were prepared to test for setting time, early hydration process, SO_4^{2-} dissolution, and compressive strength. The water–cement ratio of the cement paste specimen is 0.35 and the mixing ratio of gypsum and Mg–Al-LDH is shown in Table 1. The experiment used cement clinker without gypsum and the composition of cement clinker is shown in Table 2.

For each group of cement paste specimens, six 20 mm × 20 mm × 20 mm cubes for the compressive strength test and the early hydration process test were prepared. The standard curing age of the test piece was 3 days.

Table 1: Cement paste mix ratio design (%)

	Gypsum (%)	Mg–Al–NO_3^--LDH (%)	Mg–Al–CO_3^{2-}-LDH (%)
S2L0	2	0	0
S2L1	2	1	0
S2L3	2	3	0
S2L5	2	5	0
CS2L1	2	0	1
CS2L3	2	0	3
CS2L5	2	0	5
S3L0	3	0	0
S3L1	3	1	0
S3L3	3	3	0
S3L5	3	5	0
S3L7	3	7	0
CS3L1	3	0	1
CS3L3	3	0	3
CS3L5	3	0	5
CS3L7	3	0	7
S4L0	4	0	0
S4L1	4	1	0
S4L3	4	3	0
S4L5	4	5	0
S4L7	4	7	0
CS4L1	4	0	1
CS4L3	4	0	3
CS4L5	4	0	5
CS4L7	4	0	7

2.4 Macro performance

2.4.1 Viscosity of early hydration of cement

The viscosity of cement paste was measured by a DV-11+ viscometer from Brookfield, USA. The rotational viscometer used a No. 63 rotor, which was a cross-shaped rotor. The viscosity test program started from 15 $rad\cdot min^{-1}$ of rotation speed, increased by 15 $rad\cdot min^{-1}$ each time, took and maintained each rotation speed for 15 s, took 1 data value per second, increased logarithmically to 150 $rad\cdot min^{-1}$, and recorded the viscosity value.

2.4.2 Heat of hydration

The heat of hydration was measured using the American TAM Air eight-channel isothermal calorimeter. Each group of samples was tested with external stirring. The heat of hydration test time was 30 h. The ambient temperature

Table 2: Cement clinker composition (wt%)

Composition	SiO_2	Al_2O_3	Fe_2O_3	CaO	MgO	SO_3	K_2O	R_2O	f-CaO
	22.2	5.24	3.6	65.22	1.44	0.35	0.55	0.57	1.31

was set to 20 ± 1°C, and the reference sample was distilled water with the same specific heat.

2.5 Microstructures

2.5.1 Powdered X-ray diffraction (XRD)

The XRD diffractometer is produced by the Netherlands Panalytical Company. The copper target was used for the test. The test voltage was 40 kV and the scanning rate was 0.024°·s^{-1}. Finally, the obtained XRD patterns were analyzed by using Jade6 software to compare with the card database.

2.5.2 Thermogravimetric and differential scanning calorimetry (TG-DSC)

The TG-DSC test was performed by the SDT650 synchronous thermal analyzer produced by TA Instruments in the United States. The experimental heating rate was 10°C·min^{-1}.

2.5.3 X-ray fluorescence (XRF) surface scanning analysis

The X-ray fluorescence (XRF) surface scanning analysis was tested by Bruker-M4 Plus micro-area X-ray fluorescence spectrometer of Shanghai Boyue Instruments. The test sample was a 3 cm block with a flat surface. The test method can detect the distribution of elements on the surface of the sample.

3 Results and discussion

3.1 Mg–Al-LDH products

3.1.1 XRD results of Mg–Al–NO_3^--LDH and Mg–Al–CO_3^{2-}-LDH

The XRD results of LDH are shown in Figure 1. Based on Figure 1, there were no impurities in the synthesized Mg–Al–NO_3^--LDH and Mg–Al–CO_3^{2-}-LDH, which proved that the synthesized products were pure and correct.

3.1.2 SO_4^{2-} adsorption isotherm of Mg–Al–NO_3^--LDH and Mg–Al–CO_3^{2-}-LDH

The adsorption isotherms of SO_4^{2-} on Mg–Al–NO_3^--LDH are demonstrated in Figure 2(a) and (b). The correlation coefficients (R^2) of Langmuir and Freundlich models were 0.9999 and 0.9778, respectively. It is evident that, with the increasing initial sulfate concentration, the sulfate adsorption amount was increased dramatically and then reached equilibrium gradually. These isotherms were best fitted by the Langmuir model with higher R^2 values than the Freundlich model. A fundamental assumption of the Langmuir adsorption isotherm model is monolayer adsorption. This is consistent with the adsorption mechanism of Mg–Al–NO_3^--LDH. Thus, the isotherm adsorption behavior supports that the synthesized product is Mg–Al–NO_3^--LDH.

Mg–Al–CO_3^{2-}-LDH has no adsorption effect on SO_4^{2-}, which is in line with the anion exchange property of LDH's interlayer $CO_3^{2-} > SO_4^{2-}$. Combined with its XRD, it further corroborates that the synthesized LDH is Mg–Al–CO_3^{2-}-LDH.

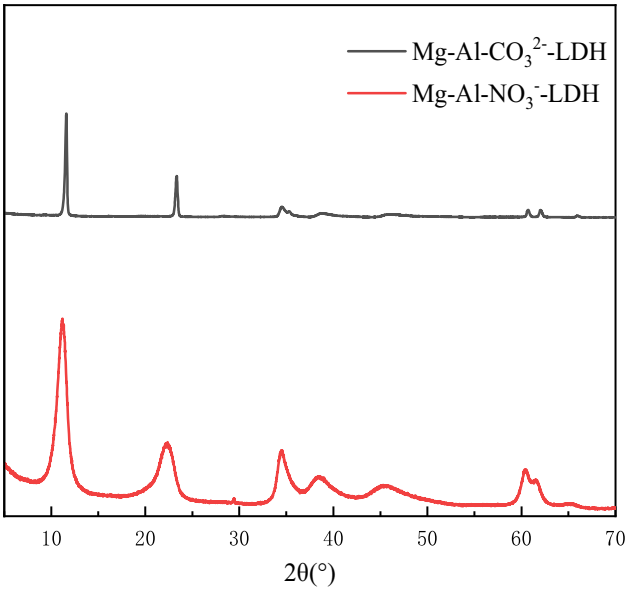

Figure 1: XRD result of Mg–Al-LDH.

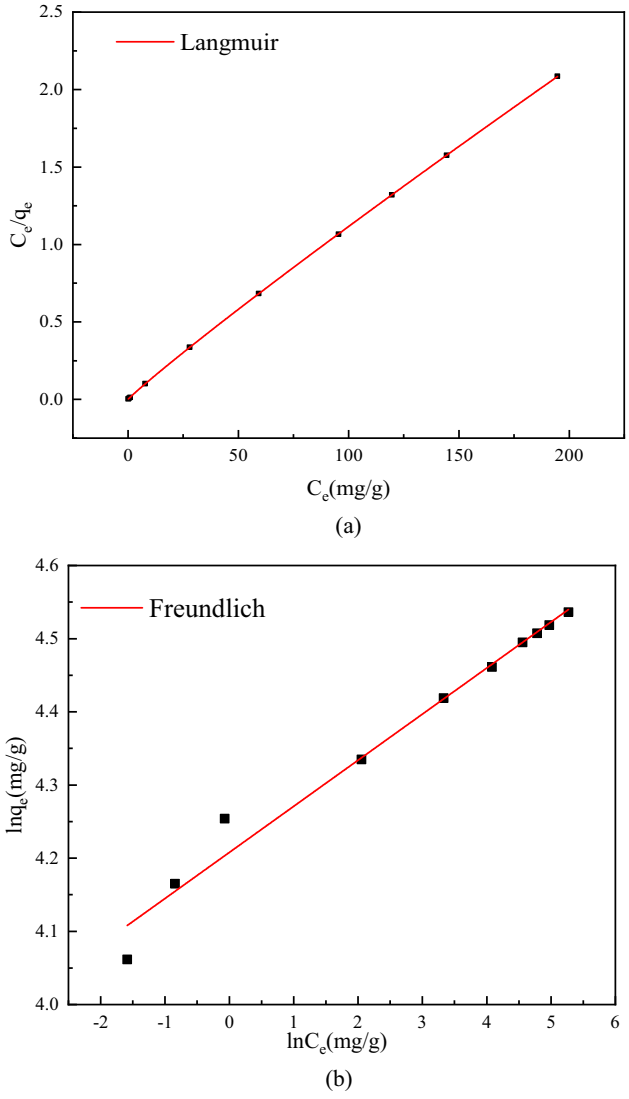

Figure 2: Adsorption isotherm experiment of Mg–Al-LDH: (a) Langmuir and (b) Freundlich.

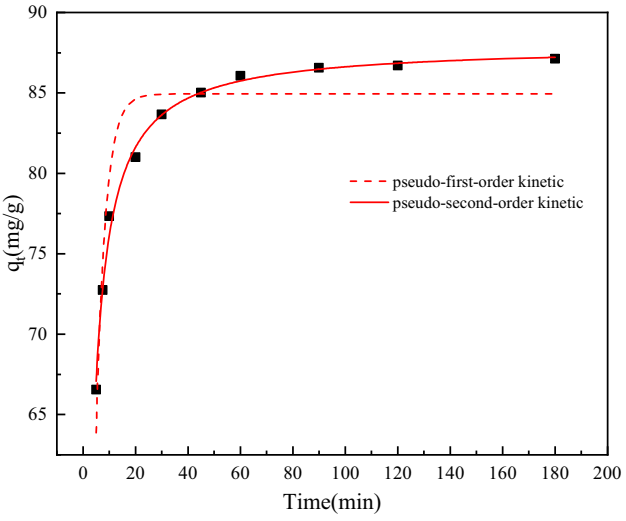

Figure 3: Adsorption kinetics experiment of LDH.

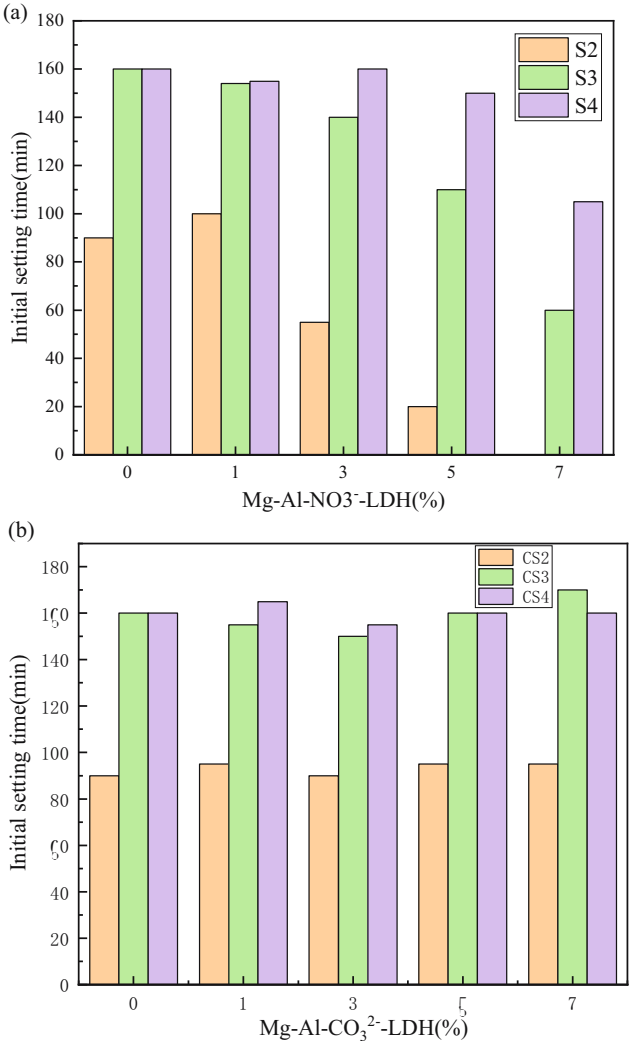

Figure 4: Initial setting time of cement paste: (a) Mg–Al–NO_3^--LDH and (b) Mg–Al–CO_3^{2-}-LDH.

3.1.3 SO_4^{2-} adsorption kinetics of Mg–Al–NO_3^--LDH and Mg – Al – CO_3^{2-}-LDH

Figure 3 shows the experimental results of adsorption kinetics of 0.2 g Mg–Al–NO_3^--LDH in the Na_2SO_4 solution. The correlation coefficients (R^2) of pseudo-first-order kinetics and pseudo-second-order kinetics were 0.8935 and 0.9947, respectively. From Figure 3, it is observed that the quasi-second-order kinetic equation can fit the experimental data well. The results showed that the adsorption capacity of SO_4^{2-} by the Mg–Al–NO_3^--LDH increased rapidly with time. Within 1 h, the adsorption capacity increased rapidly, reaching 86.06 mg·g^{-1}, which was very close to the maximum adsorption capacity. The adsorption capacity q_e = 87.97 mg·g^{-1} calculated by the pseudo-second-order kinetic equation was

close to the experimental result. This could explain that the adsorption rate is controlled by the chemisorption mechanism, including chemical reaction, electron gain or loss, or electron sharing. This result indicated that Mg–Al–NO_3^--LDH adsorbed SO_4^{2-} mainly through anion substitution.

3.2 Cement paste setting time

Figure 4(a) shows the relationship between the content of Mg–Al–NO_3^--LDH and gypsum on the setting time of cement paste. Figure 4(b) shows the relationship between the content of Mg–Al–NO_3^--LDH and gypsum on the setting time of cement paste. In this experiment, the cement paste without gypsum achieved rapid setting. The cement paste reached the initial setting state when it was transferred from the mixing pot to the setting time test mold. From Figure 4(a), when LDH was not added, the initial setting time of the cement paste is significantly prolonged when the amount of gypsum in the cement increased from 0 to 3%. However, when the gypsum content increased from 3 to 4%, the initial setting time of cement did not change significantly, which proved that the retarding effect of gypsum reached the maximum effect.

According to Figure 4(a), the initial setting time of the cement paste decreased when increasing the content of Mg–Al–NO_3^--LDH, which also showed that the retardation effect of gypsum was inhibited. However, given the same Mg–Al–NO_3^--LDH content, the initial setting time of the cement paste with 4% gypsum content was longer than that of the cement paste with 3% gypsum content. This phenomenon shed light on that the addition of Mg–Al–NO_3^--LDH would play a role in accelerating the cement paste setting, in the cement–gypsum retarding system, while an appropriate increase in the amount of gypsum would also inhibit the accelerating effect of Mg–Al–NO_3^--LDH. The retardation effect of gypsum in cement was largely due to the SO_4^{2-} released by it, but Mg–Al–NO_3^--LDH would adsorb SO_4^{2-} from gypsum, which theoretically explained the mutual inhibition between the two. Therefore, the adsorption of SO_4^{2-} by Mg–Al–NO_3^--LDH will reduce the retardation of gypsum and shorten the setting time of cement paste.

According to Figure 4(b), the incorporation of Mg–Al–CO_3^{2-}-LDH had no effect on the retardation of gypsum, compared with Figure 4(a), which can be attributed to the lack of adsorption of SO_4^{2-} by Mg–Al–CO_3^{2-}-LDH.

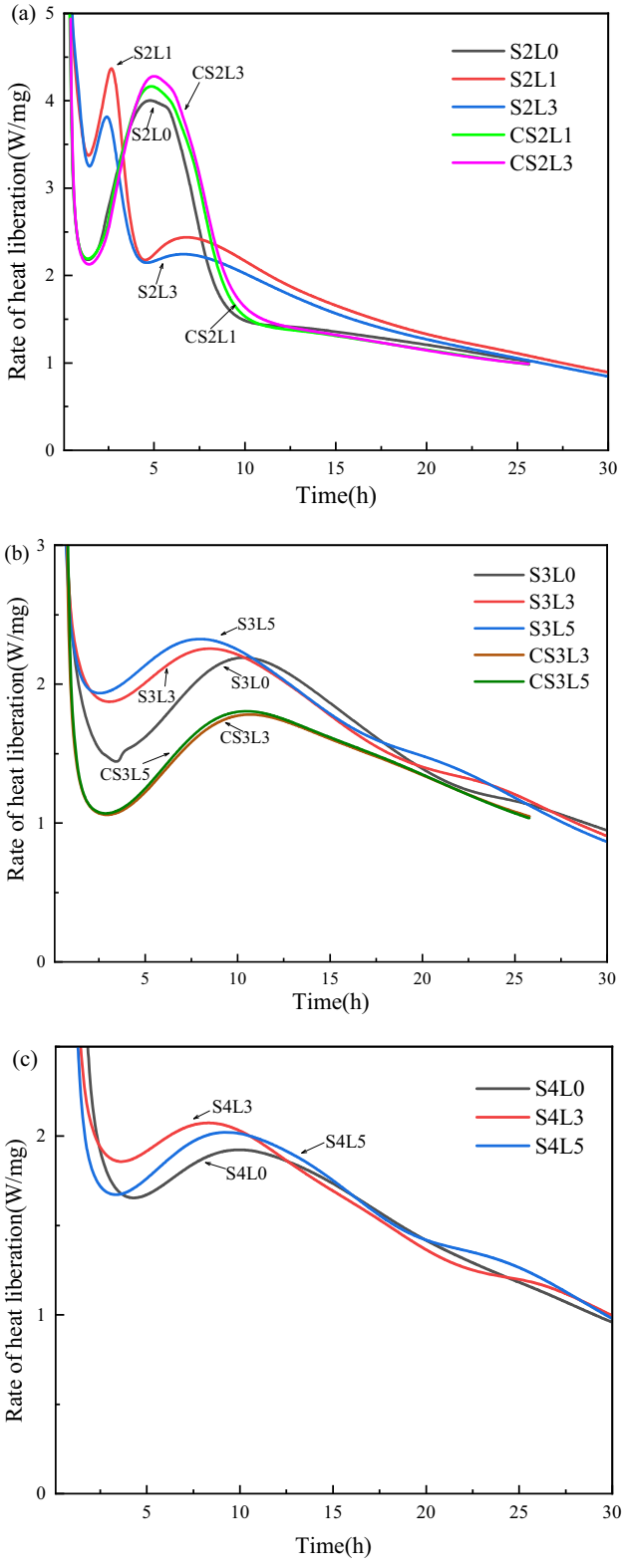

Figure 5: The results of the heat of hydration experiment: (a) 2% gypsum, (b) 3% gypsum, and (c) 4% gypsum.

3.3 Heat of hydration

The first descending phase of the hydration exothermic curve describes the dissolved exothermic release of cement particles, during which C_3A reacts with SO_4^{2-} from gypsum to produce a large amount of Aft. The first hydration exothermic peak represents the rapid formation of CSH and CH, and the cement slurry reaches the final setting state. The second hydration exothermic peak represents the reduction of SO_4^{2-} concentration in hydration products, and Aft is transformed into Afm.

Figure 5(a–c) shows the early hydration exothermic curves of cement paste with different Mg–Al-LDH contents when the gypsum content is 2, 3, and 4%, respectively. The peak corresponding time of each curve is shown in Table 3. The results of the hydration exotherm were analyzed together with the results of setting time. In the cement–gypsum retardation system, the addition of Mg–Al–NO_3^--LDH inhibits the retardation of gypsum. In the absence of Mg–Al–NO_3^--LDH, the content of 3 and 4% gypsum has the same retardation effect on cement. Nevertheless, the setting time of the cement paste with 4% gypsum content is significantly longer than that of the cement paste with 3% gypsum content, when Mg–Al–NO_3^--LDH was added.

From the time of the second exothermic reaction peak, it reflects that Mg–Al–NO_3^--LDH adsorbed SO_4^{2-} in the cement paste system, so that the concentration of SO_4^{2-} decreased, and AFt was more easily converted into AFm.

Compared with the experimental results of adding Mg–Al–CO_3^{2-}-LDH, it was known that the addition of Mg–Al–CO_3^{2-}-LDH had no obvious effect on the setting time and early hydration heat of the cement paste. It shows that the effect of Mg–Al-LDH on the hydration reaction of the cement–gypsum system is mainly due to the ion adsorption performance brought by its interlayer anion species.

3.4 Influence of Mg–Al-LDH on the viscosity of cement paste

Figure 6(a–e) shows the time-dependent viscosity change test curves of S4L0, S4L3, S4L5, CS4L3, and CS4L5, respectively. When measuring the viscosity of cement paste over time, the viscosity change curve was measured every 20 min, and the viscosity change in the cement paste within 1 h was measured in total four times, represented by −0, −1, −2, and −3. Results are plotted by selecting the viscosity data value at 45 rad·min^{-1} of the downward curve. Figure 7 provides the time-dependent change curve of the viscosity of the cement slurry with different ratios.

Each curve in Figure 6 has an upward and downward curve. The upward curve represents the test process when the rotational speed increases, and the downward curve represents the test process when the rotational speed decreases. Both the upward and downward curves show that the higher the rotational speed, the higher the viscosity.

Low shear-thinning fluid behavior, including the viscosity test curves of Mg–Al–NO_3^--LDH and Mg–Al–CO_3^{2-}-LDH, incorporated. The shear-thinning fluid behavior of the cement paste also did not change with the extension of the standing time, which proved that the incorporation of Mg–Al-LDH did not fundamentally change the fluid behavior of the cement paste.

From Figures 6(a, d, and e) and 7, the viscosity of cement pastes of S4L0, CS4L3, and CS4L5 increased noticeably with time. The shape and pattern of the test curves are similar. It can be clearly seen in Figure 7 that the incorporation of Mg–Al–CO_3^{2-}-LDH increased the viscosity of the cement paste, but the viscosity of CS4L3 and CS4L5 was not much different. The reason was that the incorporation of Mg–Al–CO_3^{2-}-LDH hinders the flow of the cement paste when the rotor rotates. However, the incorporation of Mg–Al–CO_3^{2-}-LDH did not affect the formation and change of cement hydration network structure, and did not affect the overall rheological properties of cement paste. The time-dependent changes of the three curves were similar, which proved that the rheological changes in S4L0, CS4L3 and CS4L5 were similar. From the rheological point of view, the incorporation of Mg–Al–CO_3^{2-}-LDH had little effect on the hardening of cement paste.

Table 3: The time of the hydration exothermic peak

Group	The time of first peak (h)	The time of second peak (h)
S2L0	4.93	13.72
S2L1	2.72	6.82
S2L3	2.35	6.77
CS2L1	4.87	13.82
CS2L3	5.00	13.81
S3L0	10.37	26.1
S3L3	8.47	23.78
S3L5	7.97	21.75
CS3L3	10.65	—
CS3L5	10.48	—
S4L0	9.9	—
S4L3	8.5	26.37
S4L5	9.2	24.46

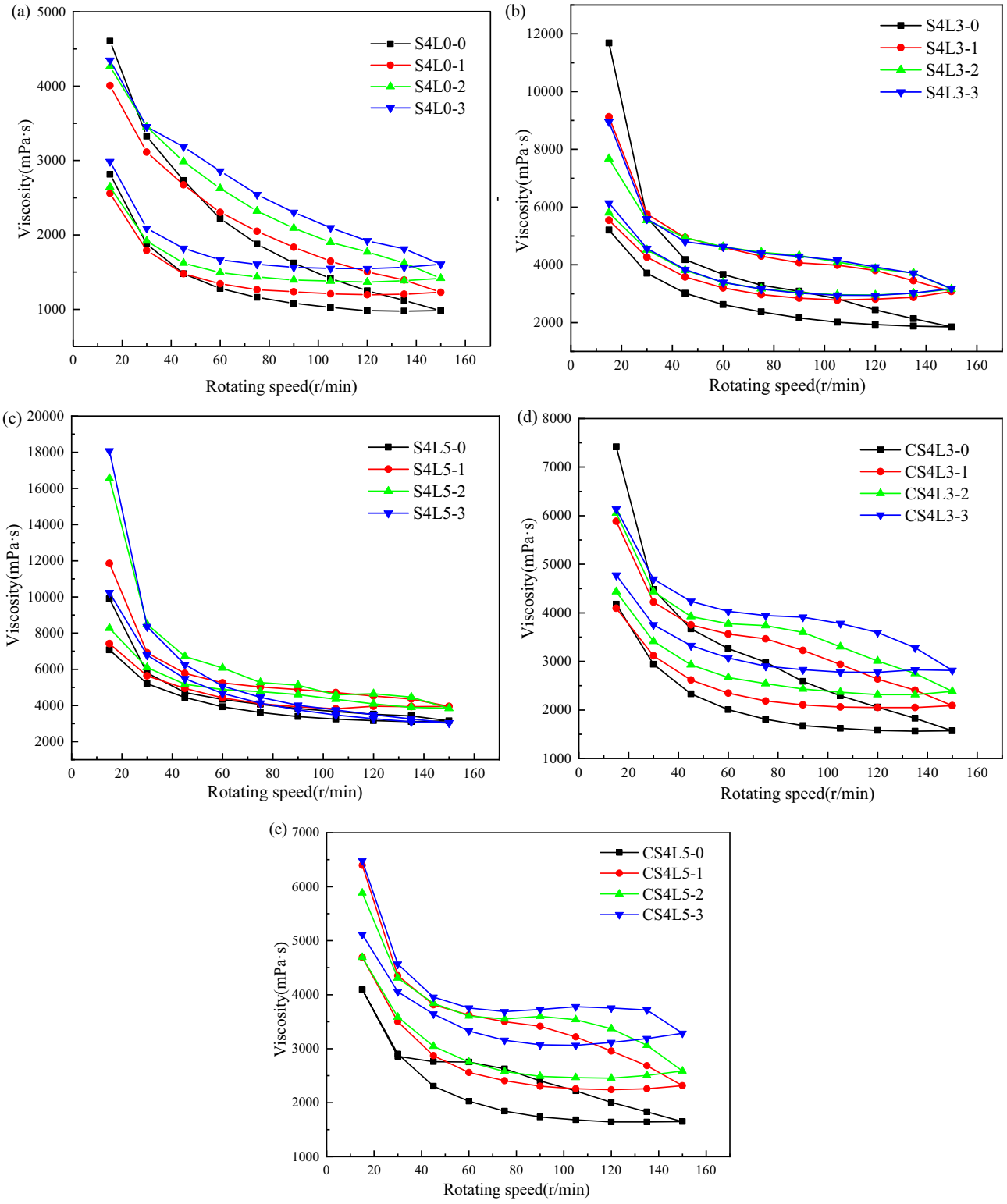

Figure 6: Viscosity test results: (a) S4L0, (b) S4L3, (c) S4L5, (d) CS4L3, and (e) CS4L5.

Figures 6 and 7 illustrate that the incorporation of Mg–Al–NO_3^--LDH increased the viscosity of the cement paste system, and the effect of the increase was much greater than that of Mg–Al–CO_3^{2-}-LDH. With an increase in the content of Mg–Al–NO_3^--LDH, the viscosity of the cement paste increased more. However, the time-dependent

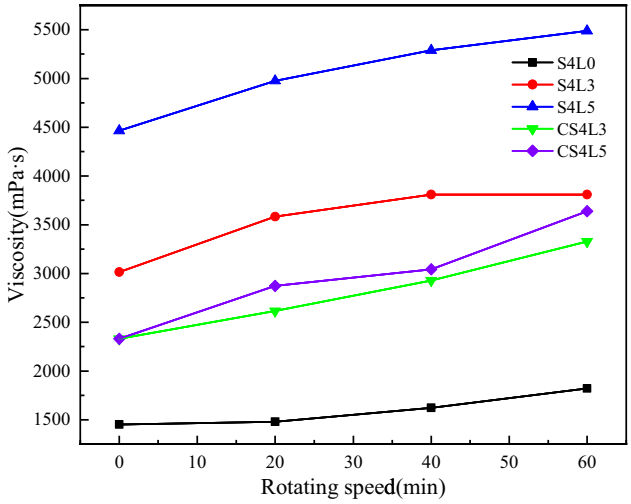

Figure 7: Experimental results of viscosity change with time.

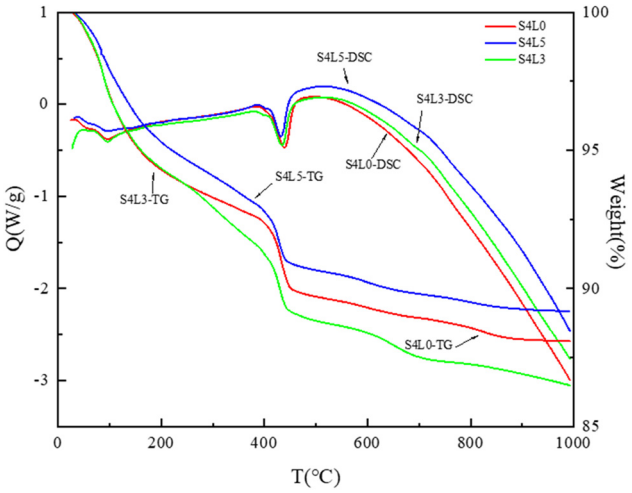

Figure 8: Experimental results of TG-DSC.

changes in S4L3 and S4L5 were different from those of S4L0. Although the viscosity of all three increases with the increase of time, their increasing trends were different.

Figure 7 clearly shows that the viscosity increase trend of S4L0 increases with time, but the viscosity increase trend of S4L3 and S4L5 tends to be flat as time increases. The incorporation of Mg–Al–NO_3^--LDH made the viscosity increase in the cement paste largely occurred in the early stage, and the viscosity growth trend slowed down after 40 min. The reason might be that the incorporation of Mg–Al–NO_3^--LDH can help the cement paste to establish a hydration structure with greater thixotropy, and the flocculation phenomenon of the cement paste was enhanced. This also explained why the S4L5-3 curve has a lower viscosity value at 150 rad·min^{-1}. Because of the flocculation effect of S4L5 cement paste, part of the water was wrapped by the flocculation structure. After a period of hydration, the flocculation structure was broken by the rotor rotation, and this part of the water was released and the viscosity of the system was reduced. However, a hydration structure network with high viscosity had been initially formed inside the cement paste system. When the rotation speed was reduced, the rotation speed was not enough to break the slurry structure again. Therefore, the viscosity of the S4L5-3 curve increased rapidly when it dropped to 15 rad·min^{-1}, and the viscosity value of the S4L5-3 exceeded the other three curve values of the S4L5.

3.5 TG-DSC results of the effect of Mg–Al-LDH on cement hydration

From the results of the cement setting time, hydration heat, and viscosity tests, it can be concluded that Mg–Al–NO_3^--LDH had an inhibitory effect on the retardation of gypsum in the cement system and shortened the time for the hydration product AFt to be converted into AFm in the cement paste. However, we need to further analyze the effect of Mg–Al–NO_3^--LDH incorporation on the early hydration of cement

The TG-DSC results of the cement system with 4% gypsum content are shown in Figure 8. According to the calculation and analysis in Figure 8, under the condition of removing the influence of Mg–Al–NO_3^--LDH content on the TG-DSC results, in the cement paste of 4% gypsum system, when the content of Mg–Al–NO_3^--LDH increases, the content of calcium hydroxide in the cement paste after hydration for 1 day decreases, and the degree of early hydration is lower. According to the previous test conclusion, the incorporation of Mg–Al–NO_3^--LDH will promote the hardening of cement paste. In the meantime, the incorporation of Mg–Al–NO_3^--LDH will reduce the degree of early cement hydration reaction, according to the TG-DSC analysis. The results showed that the hydration ranking was: S4L0 > S4L3 > S4L5.

The viscosity value test gave the reason for this phenomenon, owing to the fact that Mg–Al–NO_3^--LDH would absorb a part of the water in the aggregated cement, and the amount of water used by the mixing water for cement hydration decreased, resulting in an increase in the viscosity of the system, resulting in incomplete hydration of cement particles and reduction in the hydration process. The answers to why LDH promoted the coagulation and hardening of cement paste were that, on the one hand, it adsorbed part of the water and reduced the water–cement ratio and, on the other hand, the adsorption of SO_4^{2-} dissolved in gypsum in the cement paste system.

The incorporation of Mg–Al–NO_3^--LDH would reduce the setting time of the 4% gypsum system cement paste,

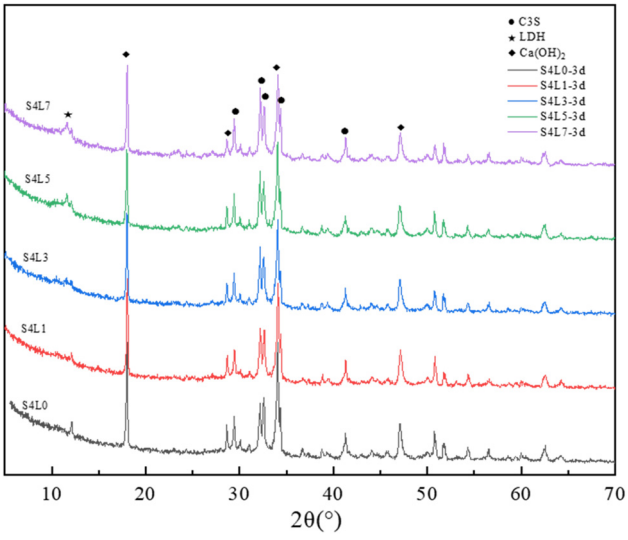

Figure 9: XRD results of the 3-day-old cement paste samples.

Table 4: 3D compressive strength of cement paste specimens

Group	Compressive strength (MPa)	Group	Compressive strength (MPa)
S2L0	34.1	S2L0	34.1
CS2L1	33.7	S2L1	32.9
CS2L3	32.5	S2L3	37.5
CS2L5	28.6	S2L5	39.3
S3L0	44.8	S3L0	44.8
CS3L1	43.5	S3L1	38.6
CS3L3	42.6	S3L3	37.9
CS3L5	38.0	S3L5	38.1
CS3L7	36.1	S3L7	41.3
S4L0	43.4	S4L0	43.4
CS4L1	43.2	S4L1	41.9
CS4L3	41.7	S4L3	39.0
CS4L5	40.5	S4L5	39.0
CS4L7	35.8	S4L7	38.7

while it reduces the early hydration degree. The more Mg–Al–NO_3^--LDH was incorporated, the greater the effect.

3.6 XRD results of the effect of Mg–Al-LDH on cement hydration

Figure 9 shows the XRD results of the 3-day-old cement paste samples. From Figure 10, with the increase in the Mg–Al–NO_3^--LDH content, the diffraction peak of Mg–Al–NO_3^--LDH became more obvious; however, the content of CH was gradually decreasing. With the increase in the Mg–Al–NO_3^--LDH dosage, the peak intensity of C_3S is higher. This showed that the hydration ranking was S4L0 > S4L1 > S4L3 > S4L5 > S4L7.

3.7 Early compressive strength results of cement paste specimens

The 3-day compressive strength results of the cement paste specimens are shown in Table 4. Regardless of the content of gypsum, the early compressive strength of the

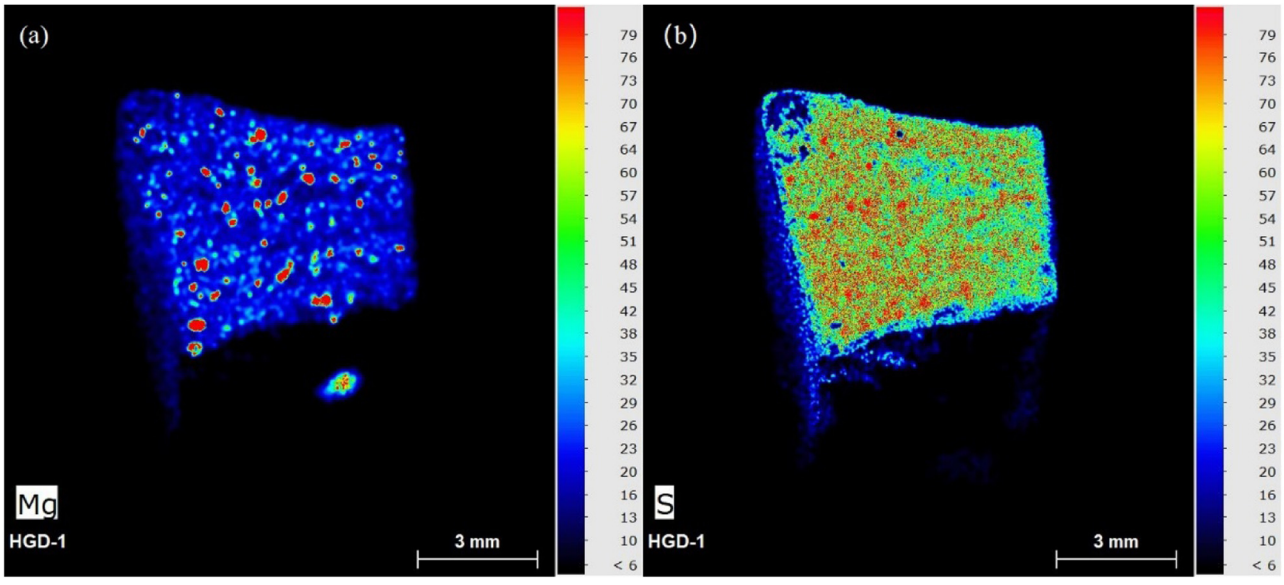

Figure 10: XRF scan result of S3L5: (a) Mg and (b) S.

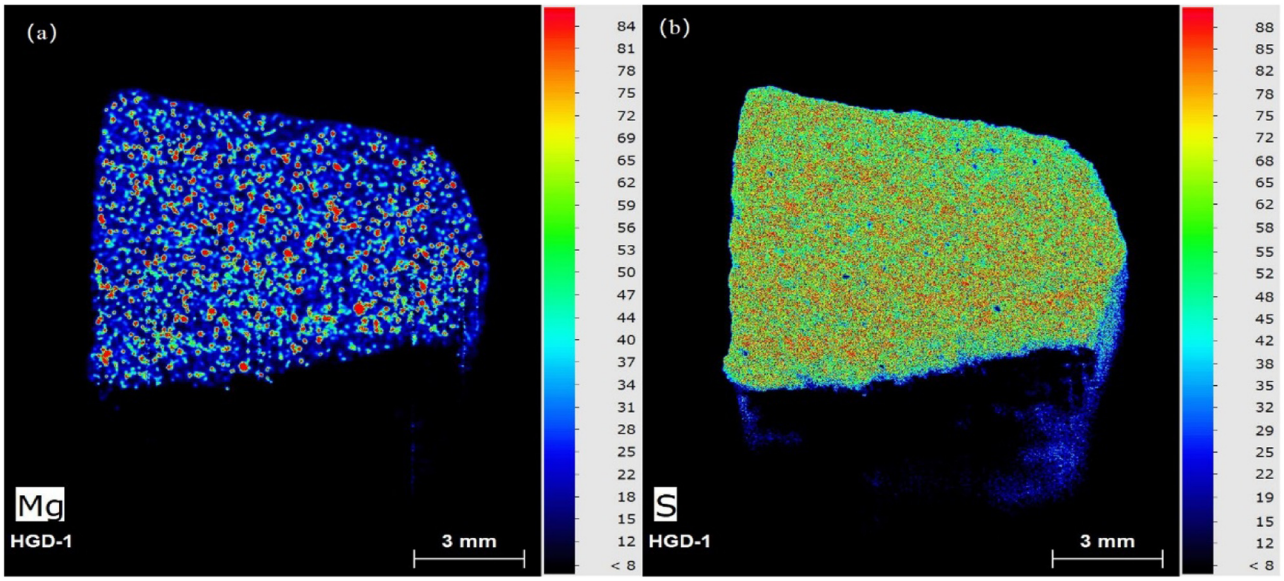

Figure 11: XRF scan result of CS3L5: (a) Mg and (b) S.

cement paste specimens decreased with the increase in the content of $Mg-Al-CO_3^{2-}$-LDH. The reason for the reduction in compressive strength was that $Mg-Al-CO_3^{2-}$-LDH did not participate in the cement hydration reaction but created an additional interfacial weakness in the specimen.

It can be seen that under the condition of 4% gypsum content, the compressive strength of the specimen decreased with the increase in the Mg–Al–NO_3^--LDH content, this phenomenon was consistent with the previous experimental results. According to the previous experiments, we know that the reason for why Mg–Al–NO_3^--LDH reduced the degree of hydration reaction was that it would adsorb free water used to participate in the hydration reaction. Because, at 4% gypsum content, the cement paste mixed with Mg–Al–NO_3^--LDH also could maintain a longer setting time. However, under the condition of 2 and 3% gypsum content, the addition of Mg–Al–NO_3^--LDH would greatly reduce the setting and hardening time of the cement paste so that the free water content in the cement paste would decrease rapidly. With the rapid reduction in free water content in the hydration reaction system, Mg–Al–NO_3^--LDH would release the adsorbed free water. Therefore, in the early hydration reaction, the unhydrated cement particles had enough water for the hydration reaction, which reduced the early negative influence of Mg–Al–NO_3^--LDH on the hydration reaction. When Mg–Al–NO_3^--LDH rapidly released free water, it played a role in promoting the coagulation of the cement paste so that the early hydration degree of the paste sample would be improved. This was the reason for the phenomenons of S2L5 > S2L3 > S2L1 > S2L0 and S3L7 > S3L5. The experimental results confirmed that the effect of Mg–Al–NO_3^--LDH on the hydration of cement paste was related to the gypsum content in the cement paste.

3.8 Results of the XRF surface scan

Figure 10(a) and (b) shows the XRF scan result of S3L5. The area where the Mg element is obvious is Mg–Al–NO_3^--LDH, and the area where the S element is obvious is SO_4^{2-}. Figure 10(a) represents the distribution of Mg elements, and Figure 11(b) represents the distribution of S elements. From the figure, in the S3L5 specimen, SO_4^{2-} will gather near the Mg–Al–NO_3^--LDH. Therefore, it is evident that in the cement paste, Mg–Al–NO_3^--LDH will adsorb the SO_4^{2-} dissolved in gypsum.

Figure 11(a) and (b) shows the XRF scan result of CS3L5. It can be mentioned from Figure 11(a) and (b) that SO_4^{2-} was evenly distributed in the specimen and did not aggregate near $Mg-Al-CO_3^{2-}$-LDH, which proved that $Mg-Al-CO_3^{2-}$-LDH did not adsorb SO_4^{2-} in the cement paste. This phenomenon is consistent with the anionic adsorption performance of Mg–Al-LDH(CO_3^{2-} > SO_4^{2-} > OH^- > F^- > Cl^- > Br^- > NO_3^-).

4 Conclusion

This research investigated the combined effect of Mg–Al-LDH and SO_4^{2-} from gypsum on the early hydration of

cement in the cement paste by testing the setting time, hydration heat, viscosity of cement paste with different ratios, and XRD, TG-DSC, compressive strength, and XRF surface scan of cement paste specimens with different ratios. Based on the presented results, the following conclusions can be drawn:

1. In the gypsum-cement system, the addition of Mg–Al–NO_3^--LDH will shorten the setting time of the cement paste and advance the time of the hydration exothermic peak, which will make the hydration product AFt more easily converted into AFm.
2. The addition of Mg–Al–NO_3^--LDH did not change the shear-thinning rheological properties of the cement paste; nonetheless, it enhanced the flocculation effect of the cement paste and increased the viscosity of the cement paste. With the addition of Mg–Al–NO_3^--LDH, the viscosity growth law of the cement paste changed with time.
3. In cement system with different gypsum contents, the incorporation of Mg–Al–NO_3^--LDH has a different influence on cement hydration
4. Mg–Al–NO_3^--LDH will adsorb SO_4^{2-} dissolved from gypsum in the cement–gypsum system. This phenomenon supports that SO_4^{2-} in the cement–gypsum system would reduce the effect of Mg–Al–NO_3^--LDH on improving the corrosion resistance of the specimen due to its adsorption capacity.
5. Mg – Al – CO_3^{2-}-LDH has no obvious effect on the setting time, viscosity, and hydration of cement. But it will exist as a defect and reduce the compressive strength of cement specimens.
6. In future studies, the effect of Mg–Al-LDH on the erosion resistance of sulfoaluminate cement remains to be investigated.

Funding information: This research was funded by the "National Natural Science Foundation of China" No. 52178196. This research was also supported by "State Key Laboratory of Solid Waste Reuse for Building Materials" SWR-2020-005.

Author contributions: Zedong Qiu: Formal analysis, Data curation, Methodology, Validation, Writing – original draft. Lim Limin Deng: Methodology, Validation, Funding acquisition. Shuang Lu: Conceptualization, Supervision, Validation, Writing – review & editing, Funding acquisition. Guoqiang Li: Investigation, Data curation, Project administration. Zhen Tang: Conceptualization, Supervision.

Conflict of interest: The authors declare no conflict of interest regarding the publication of this study.

References

[1] Tang, Z., Z. D. Qiu, S. Lu, and X. Shi. Functionalized layered double hydroxide applied to heavy metal ions absorption: A review. *Nanotechnology Review*, Vol. 9, No. 1, 2020, pp. 800–819.
[2] Liang, L. and L. Li. Adsorption behavior of calcined layered double hydroxides towards removal of iodide contaminants. *Journal of Radioanalytical and Nuclear Chemistry*, Vol. 273, 2007, id. 1.
[3] Miyata, S. Anion-exchange properties of hydrotalcite-like compounds. *GeoScienceWorld*, Vol. 31, 1983, id. 4.
[4] Zhang, Y., J. Liu, Y. Li, M. Yu, S. Li, and B. Xue. Fabrication of inhibitor anion-intercalated layered double hydroxide host films on aluminum alloy 2024 and their anticorrosion properties. *Journal of Coatings Technology and Research*, Vol. 12, No. 2, 2015, pp. 293–302.
[5] Kuang, Y., L. Zhao, S. Zhang, F. Zhang, M. Dong, and S. Xu. Morphologies, preparations and applications of layered double hydroxide micro-/nanostructures. *Materials*, Vol. 3, No. 12, 2010, pp. 5220–5235.
[6] Ma, J., P. Duan, D. Ren, and W. Zhou. Effects of layered double hydroxides incorporation on carbonation resistance of cementitious materials. *Journal of Materials Research & Technology*, Vol. 8, No. 1, 2019, pp. 292–298.
[7] Ke, X., S. A. Bernal, and L. Provis John. Uptake of chloride and carbonate by Mg-Al and Ca-Al layered double hydroxides in simulated pore solutions of alkali-activated slag cement. *Cement and Concrete Research*, Vol. 100, 2017, pp. 1–13.
[8] Shui, Z., J. Ma, and W. Chen. Chloride binding capacity of cement paste containing layered double hydroxide (LDH). *Journal of Testing and Evaluation: A Multidisciplinary Forum for Applied Sciences and Engineering*, Vol. 40, 2012, id. 5.
[9] Yang, Z., F. Hartmut, and P. Rob. Laboratory investigation of the influence of two types of modified hydrotalcites on chloride ingress into cement mortar. *Cement & Concrete Composites*, Vol. 58, 2015, pp. 105–113.
[10] Xu, J., Y. Song, Y. Zhao, L. Jiang, Y. Mei, and P. Chen. Chloride removal and corrosion inhibitions of nitrate, nitrite-intercalated Mg Al layered double hydroxides on steel in saturated calcium hydroxide solution. *Applied Clay Science*, Vol. 163, 2018, pp. 129–136.
[11] Tatematsu, H. and T. Sasaki. Repair materials system for chloride-induced corrosion of reinforcing bars. *Cement & Concrete Composites*. Vol. 25, No. 1, 2003, pp. 123–129.
[12] Qu, Z. Y., Q. L. Yu, and H. J. Brouwers. Relationship between the particle size and dosage of LDHs and concrete resistance against chloride ingress. *Cement and Concrete Research*, Vol. 105, 2018, pp. 81–90.
[13] Wu, Y., P. Duan, and C. Yan. Role of layered double hydroxides in setting, hydration degree, microstructure and compressive strength of cement paste. *Applied Clay Science*, Vol. 158, 2018, pp. 123–131.
[14] Ping, D., W. Chen, J. Ma, and Z. Shui. Influence of layered double hydroxides on microstructure and carbonation resistance of sulphoaluminate cement concrete. *Construction and Building Materials*, Vol. 48, 2013, pp. 601–609.
[15] Shui, Z. H., R. Yu, Y. X. Chen, P. Duan, J. T. Ma, and X. P. Wang. Improvement of concrete carbonation resistance based on

a structure modified Layered Double Hydroxides (LDHs): Experiments and mechanism analysis. *Construction & Building Materials*, Vol. 176, 2018, pp. 228–240.

[16] Cao, Y., D. Zheng, S. Dong, F. Zhang, J. Lin, C. Wang, et al. A composite corrosion inhibitor of MgAl layered double hydroxides co-intercalated with hydroxide and organic anions for carbon steel in simulated carbonated concrete pore solutions. *Journal of The Electrochemical Society*, Vol. 166, No. 11, 2019, pp. C3106–C3113.

[17] Yoon, S., J. Moon, S. Bae, X. Duan, E. P. Giannelis, and P. M. Monteiro. Chloride adsorption by calcined layered double hydroxides in hardened Portland cement paste. *Materials Chemistry & Physics*, Vol. 145, No. 3, 2014, pp. 376–386.

[18] Xu, S., Z. Chen, B. Zhang, J. Yu, F. Zhang, and D. G. Evans. Facile preparation of pure CaAl-layered double hydroxides and their application as a hardening accelerator in concrete. *Chemical Engineering Journal*, Vol. 155, No. 3, 2009, pp. 881–885.

[19] Chen, Y., R. Yu, X. Wang, X. Chen, and Z. Shui. Evaluation and optimization of ultra-high performance concrete (UHPC) subjected to harsh ocean environment: Towards an application of layered double hydroxides (LDHs), *Construction and Building Matetials*, Vol. 177, 2019, pp. 51–62.

[20] Haiyan, L. I., G. Xuemao, L. Yang, S. Liu, J. Zhang, and Y. Guo. Effects of LiAl-layered double hydroxides on early hydration of calcium sulphoaluminate cement paste. *Journal of Wuhan University of Technology-Materials Science Education*, Vol. 32, No. 5, 2017, pp. 1101–1107.

[21] Li, R., Q. Yue, F. Shen, R. Qin, G. Zhang, Z. Li, et al. Adsorption of aqueous mercury(II) by thiol-modified cron stalk. *Fresenius Environmental Bulletin*, Vol. 22, No. 1, 2013, pp. 178–185.